Ultrahigh extinction ratio silicon micro-ring modulator by MDM resonance for high speed PAM modulation

Jiacheng Liu[1], Jiangbing Du[1, 2, *], Weihong Shen[1], Gangqiang Zhou[1], Linjie Zhou[1], Ke Xu[3], and Zuyuan He[1, 2]
[1]*State Key Laboratory of Advanced Optical Communication Systems and Networks, Shanghai Jiao Tong University, Shanghai 200240, China.*
[2]*Peng Cheng Laboratory*
[3]*Department of Electronic and Information Engineering, Harbin Institute of Technology (Shenzhen), Shenzhen 518055, China*
**dujiangbing@sjtu.edu.cn*

Abstract: Silicon micro-ring modulator assisted by MDM resonance is experimentally demonstrated. Ultrahigh ER up to 55 dB was obtained for supporting 50 Gb/s PAM4 signaling with 0.79-V·cm $V_{\pi}L$, indicating promising performance for advanced modulation formats. © 2022 The Author(s)

1. Introduction

Silicon modulator with high power efficiency and high-speed is a key building block of silicon photonics, a promising technology to overcome the bottleneck of current electrical interconnect systems. Currently, Mach-Zehnder modulator (MZM) and micro-ring modulator (MRM) are two main kinds of modulators that are widely used. Compared with MZM, MRM has some unique advantages such as small footprint, intrinsic wavelength-division-multiplexing (WDM) compatibility, simpler driver architecture and low power consumption [1]. During the past few years, silicon MRM has been extensively studied with data rates up to 128 Gb/s [2-3] using on-off keying (OOK) modulation. Higher data rates up to 200 Gb/s were demonstrated by using four-level pulse-amplitude-modulation (PAM4) [4-6]. Extinction ratio (ER) of the micro-ring resonator is of vital importance in PAM modulation. It depends on the relative magnitude of the micro-ring loss coefficient and transmission coefficient. The loss coefficient mainly relies on the absorption loss of the free carrier and is hard to control, thus makes it very difficult to obtain high ER for MRM. Currently, The ER for silicon MRM is generally limited at about 20 dB level, which highly limits the performance of advanced modulation formats.

In this work, we presented a mode-division-multiplexing (MDM) resonance enhanced silicon micro-ring modulator to trap the light twice within single micro-ring resonator by using different optical modes. L-shaped PN junction was utilized to provide efficient modulation for both TE_0 and TE_1 modes. Ultrahigh ER up to 55 dB was obtained and 50 Gb/s PAM4 modulation was experimentally demonstrated.

2. Device structure and working principle

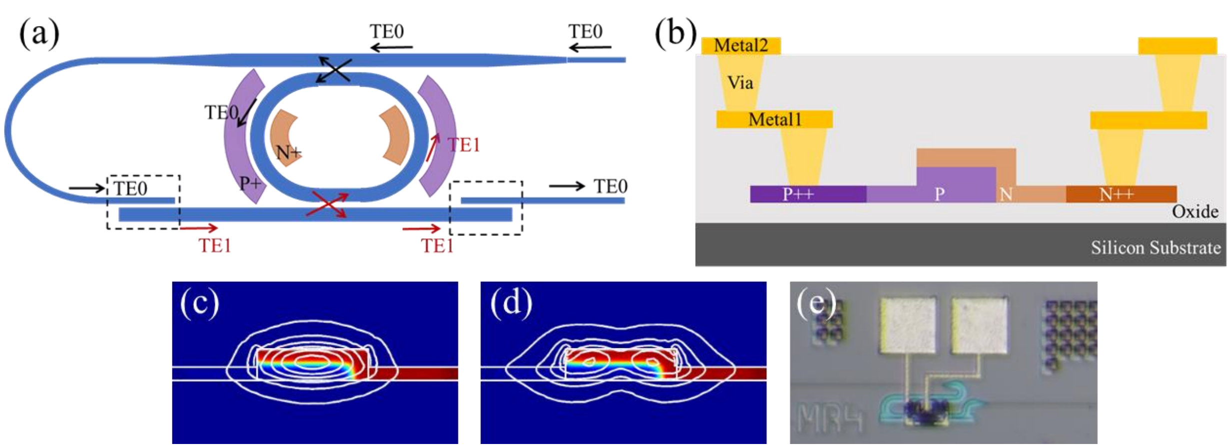

Fig. 1. (a) Schematic structure of the proposed modulator. (b) Cross-section of the modulator phase shifter. (c) TE_0 and (d) TE_1 mode overlap with L-shaped PN junction. (e) Microscope image of the proposed modulator.

Fig. 1(a) shows the schematic structure of the proposed device. It is shown that the modulator is composed of a micro-ring resonator and two mode converters. The waveguide width of the micro-ring modulator is 930 nm, supporting TE_0 and TE_1 mode. The mode converter was designed based on asymmetric directional coupler (ADC) structure with a

5.5 μm coupling length. The input light first couples into the two-mode micro-ring resonator in TE_0 mode after passing through a tapered region. The TE_0 mode resonates within the ring and output from the through port. Afterwards, the output TE_0 mode is converted to TE_1 mode by an asymmetric directional coupler (ADC) mode converter and coupled again into the micro-ring in TE_1 mode. After resonating in the ring, the light converts back to TE_0 mode by an identical mode converter and finally outputs. Both the TE_0 and TE_1 mode are phase modulated in the two-mode micro-ring resonator by an L-shaped PN junction with high modulation efficiency.

Fig. 1(b) shows the cross-section structure of the phase shifter within the micro-ring modulator. The waveguide width is 930 nm and the height is 220 nm with a 90-nm slab. An L-shaped PN junction is formed in the cross-section of the two-mode waveguide. Both the TE_0 and TE_1 mode are phase modulated with high efficiency thanks to the large overlap between the depletion region of the L-shaped PN junction and the optical mode. The TE_0 and TE_1 mode overlap with the L-shaped PN junction are shown in Fig. 1(c) and (d) respectively. The doping concentration is 1×10^{18} cm-3 for the p-type region and 8×10^{17} cm-3 for the n-type region. The heavily doped n-type and p-type concentrations are 1×10^{20} cm-3. The heavily doped region is 500 nm away from the edge of the waveguide. The device was fabricated via a standard silicon photonic processing project provided by Advanced Micro Foundry (AMF), Singapore. The microscope image of the fabricated device is shown in Fig. 1(e).

3. Device characterization

The static transmission spectrum was first measured by using a tunable CW laser (Santec TSL-710) and a photodetector. The result is shown in Fig. 2(a). From the figure, we can clearly see that the transmission spectrum is the summation of two resonance curves with different free spectral range (FSR). One comes from the TE_0 mode and the other comes from the TE_1 mode. The resonance curve of TE_0 mode has a smaller full width half maximum (FWHM) while the FWHM of TE_1 is larger because of its higher transmission loss in the resonator. The peak of two resonance curves finally meet each other at 1572.7 nm leaving a sharp resonance peak with 40 dB static extinction ratio. The transmission spectrum under different reverse bias voltages is shown in Fig. 2(b). Record high extinction ratio reaches 55 dB at -2 V bias voltage. The resonance shift is 49 pm/V corresponding to a modulation efficiency of 0.79 V·cm.

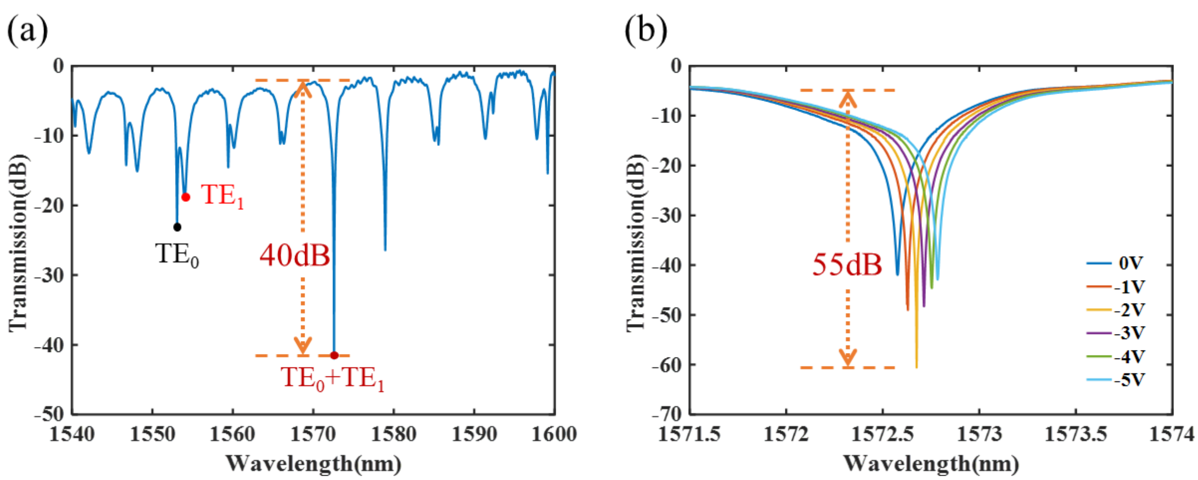

Fig. 2. (a) Measured transmission spectrum of the modulator. (b) Transmission spectrum under various reverse bias voltages.

To verify the high-speed performance of the proposed modulator, we set up the high-speed measurement for the modulator. The experiment setup for the high-speed measurement is shown in Fig. 3. The CW laser source is tuned near 1572.7 nm with 10 dBm output power. A 2^7-1 pseudo-random binary sequence (PRBS) signal was generated from a 64-GSa/s arbitrary wave generator (AWG, Keysight, M8192A) and amplified by an RF amplifier (SHF807C). The RF signal is combined with -3V DC bias by a bias-tee and loaded onto the modulator. The DC voltage is applied to adjust the proper operation point of the modulator. The modulated optical signal is amplified via EDFA and then received by a high-speed photodetector and a real-time oscilloscope for off-line digital signal processing (DSP).

We carried out high-speed data transmission by using PAM4 and PAM8 modulation format. The BER curves of the 40 Gb/s PAM4, 50 Gb/s PAM4 and 30 Gb/s PAM8 signals are plotted in Fig. 4(a). The 40 Gb/s PAM4 signal has a BER under 7% forward error correction (FEC) threshold (3.8e-3) at >-1 dBm received optical power, and the 50

Gb/s PAM4 signal has a BER under 7% FEC at >0 dBm power. For the 30 Gb/s PAM8 signal, it has a BER under 20% FEC threshold (2e-2) at >1 dBm power. Fig. 4(b)-(d) shows the corresponding post-FFE eye diagrams of 40 Gb/s PAM4, 50 Gb/s PAM4 and 30 Gb/s PAM8 respectively.

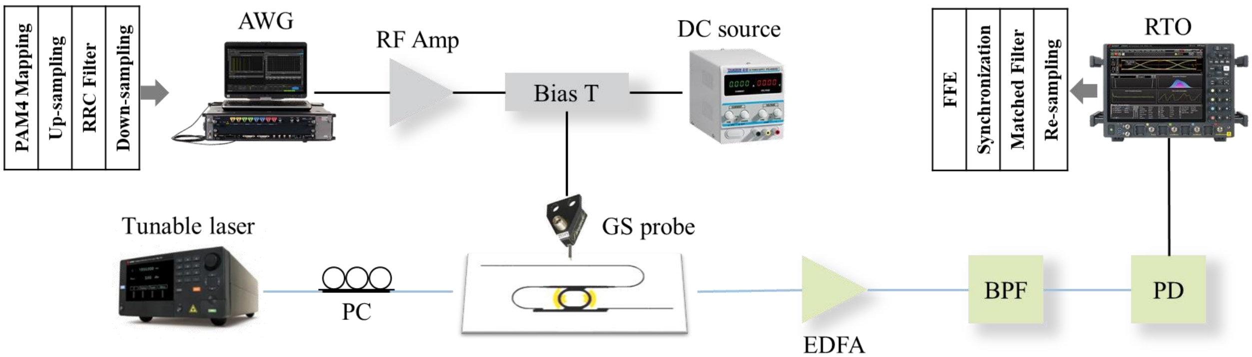

Fig. 3. Schematic diagram of the high-speed measurement setup.

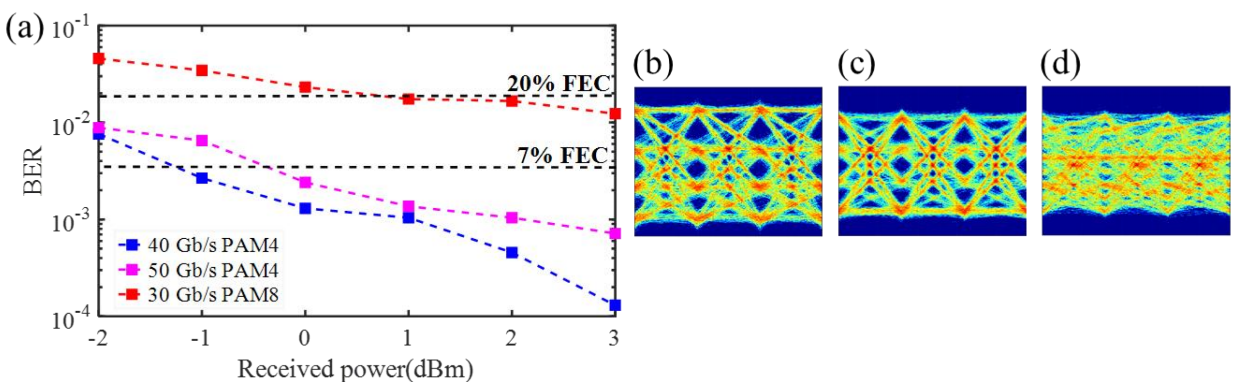

Fig. 4. (a) BER curves of 40 Gb/s, 50 Gb/s PAM4 and 30 Gb/s PAM8 signals. (b) Off-line post-FFE eye diagrams of 40 Gb/s PAM4 (c) 50 Gb/s PAM4 and (d) 30 Gb/s PAM8 with the lowest BERs.

4. Conclusion

We proposed and experimentally demonstrated a MDM resonance enhanced silicon micro-ring modulator. Ultrahigh extinction ratio of 55 dB was realized by resonating the light twice within the micro-ring resonator with different modes. 50-Gb/s PAM4 modulation with BER under 7% FEC was experimentally demonstrated. The high extinction ratio benefits the performance of high-speed PAM signals and we believed that it will pave the way towards the realization of higher order modulation formats by using micro-ring modulator.

Acknowledgement

National Natural Science Foundation of China (NSFC) (61935011, 61875124, 61875049); The Major Key Project of PCL(PCL2021A1).

5. References

[1] J. Sun, et al, J. Lightwave Technol. 37, 110-115 (2019)
[2] M. Pantouvaki, et al, J. Lightwave Technol. 35, 631-638 (2017)
[3] M. Sakib, et al, CLEO 2021, paper SF1C.3.
[4] H. Li, et al, J. Lightwave Technol. 38, 131-138 (2020)
[5] Y. Zhang, et al, ECOC 2020, paper 1-4.
[6] X. Wu, et al, Opt. Express 28, 26492-26498 (2020)